Available online at www.sciencedirect.com
ScienceDirect
Trans. Nonferrous Met. Soc. China 28(2018) 1553−1562
Transactions of Nonferrous Metals Society of China
www.tnmsc.cn

Bioactivity, in-vitro corrosion behavior, and antibacterial activity of silver−zeolites doped hydroxyapatite coating on magnesium alloy

H. R. BAKHSHESHI-RAD[1,2], E. HAMZAH[2], A. F. ISMAIL[3], M. AZIZ[3], E. KARAMIAN[1], N. IQBAL[4]

1. Advanced Materials Research Center, Department of Materials Engineering, Najafabad Branch, Islamic Azad University, Najafabad, Iran;
2. Department of Materials, Manufacturing and Industrial Engineering, Faculty of Mechanical Engineering, Universiti Teknologi Malaysia, 81310 Johor Bahru, Johor, Malaysia;
3. Advanced Membrane Technology Research Center (AMTEC), Universiti Teknologi Malaysia, 81310 Skudai, Johor Bahru, Johor, Malaysia;
4. Department of Biomedical Engineering, University of Engineering and Technology, Lahore, Pakistan

Received 4 August 2017; accepted 14 February 2018

Abstract: Mg-based alloys received significant attention for temporary implant applications while, their applications have been limited by high degradation rate. Therefore, silver−zeolite doped hydroxyapatite (Ag−Zeo−HAp) coating was synthesized on TiO_2-coated Mg alloy by physical vapour deposition (PVD) assisted electrodeposition technique to decrease the degradation rate of Mg alloy. X-ray diffraction (XRD) analysis and field emission scanning electron microscopy (FE-SEM) images showed the formation of a uniform and compact layer of Ag−Zeo−HAp with a thickness of 15 μm on the TiO_2 film with a thickness of 1 μm. The potentiodynamic polarization (PDP) and electrochemical impedance spectroscopy (EIS) tests indicated that corrosion resistance of Mg−Ca alloy was considerably increased by the Ag−Zeo−HAp coating. The bioactivity test in the simulated body fluid (SBF) solution showed that a dense and homogeneous bonelike apatite layer was formed on the Ag−Zeo−HAp surface after 14 d. Investigation of antibacterial activity via disk diffusion and spread plate methods showed that the Ag−Zeo−HAp coating had a significantly larger inhibition zone (3.86 mm) towards *Escherichia coli* (*E. coli*) compared with the TiO_2-coated Mg alloy (2.61 mm). The Ag−Zeo−HAp coating showed high antibacterial performance, good bioactivity, and high corrosion resistance which make it a perfect coating material for biomedical applications.

Key words: magnesium alloy; zeolite; coating; bioactivity; corrosion behavior; antibacterial activity

1 Introduction

Recently, magnesium alloys have received considerable attention among the potential metallic implants because of their desirable characteristics such as extremely light weight, outstanding mechanical properties close to those of the natural bone, ability to degrade in-vivo, and excellent biocompatibility [1−4]. In addition, Mg will be able to control bone proliferation and remodelling due to its engagement in the bone mineral surface reaction [5,6]. Moreover, the presence of Mg^{2+} in apatite crystals may increase the speed of osteoblast adhesion and enhance bone formation [5−7]. However, Mg alloys exhibited poor corrosion resistance particularly in the physiological solution, which limited their extensive use in biomedical applications [8−10]. To enhance the corrosion resistance of Mg alloys, besides surface modification, element alloying was established for protection of Mg alloys [11]. In this context, SUN et al [12] showed that the corrosion resistance of Mg alloy increased with combination of alloying and surface treatment. The main alloying elements are Ca, Zn, Mn, Si, Sr, Li and RE which were added to Mg alloy in order to improve its corrosion resistance [13]. In this respect, ZENG et al [13] showed that Mg–0.79Ca alloy presented higher mechanical properties and lower corrosion rate than Mg−0.54Ca and Mg−1.35Ca alloys, due to the microstructure homogeneity. Similarly, CUI et al [14] showed that MAO-coated Mg−0.79Ca alloys exhibited higher corrosion resistance compared with the Mg−0.54Ca and Mg−1.35Ca alloys. In order to further

Corresponding author: H. R. BAKHSHESHI-RAD; E-mail: rezabakhsheshi@gmail.com; rezabakhsheshi@pmt.iaun.ac.ir
DOI: 10.1016/S1003-6326(18)64797-1

enhance corrosion resistance, HAp-based nanocomposite materials have been deposited on Mg alloy. Hydroxyapatite (HAp, $Ca_{10}(PO_4)_6(OH)_2$) is generally employed as a coating material in biomedical applications for increasing the corrosion resistance, biocompatibility, and osteoconductive properties, although HAp presented poor antibacterial performance [7,15]. The addition of trace amount of Ag, Zn, Ti, and Cu ions into HAp structures enhances their antimicrobial performance [16,17]. Zeolites (Zeo) are a kind of crystalline nanoporous aluminosilicates with great mechanical and chemical stability which present good corrosion protection [8,16−18]. Zeo is also nontoxic and contains metal ions like sodium or calcium [17]. These metal ions are able to exchange with metals including Ag and Zn ions for further improvement of antibacterial performance [19]. Zeolite coating has corrosion resistance in the presence of various organic acids, such as acetic acid, formic acid and citric acid. For example, KATARIYA et al [20] also investigated the effect of ZSM-5 zeolite coating on the corrosion behavior of mild steel in mineral acids and their results exhibited that corrosion inhibition efficiency increased to 98% after ZSM-5 zeolite coating. SONG et al [8] coated ZSM-5 zeolite on Mg−Li alloy via hot-pressing method and their results showed that ZSM-5 zeolite coated alloy presented better corrosion resistance than bare Mg alloy. BANERJEE et al [21] demonstrated that protective performance of zeolite-coated Mg alloy is significantly higher than that of uncoated Mg alloy in NaCl solution. CUI et al [22] prepared polymethyltrimethoxysilane (PMTMS)/titania (TiO_2) composite on the Mg alloy surface and their results showed that corrosion rate of composite coating is significantly lower than that of Mg alloy substrate. ZENG et al [23] prepared cerium-doped zinc calcium phosphate film on the surface of Mg alloy and their results demonstrated that deposited film is able to effectively protect the AZ31 Mg substrate. Likewise, PHUONG et al [24] illustrated that magnesium phosphate conversion coating on Mg alloy decreases corrosion current of bare sample. LI et al [25] exhibited that the corrosion resistance of the AZ31 Mg alloy was increased considerably via coating containing dicalcium phosphate dihydrate (DCPD). WANG et al [26] depicted that Ca-deficient hydroxyapatite coating reduces the degradation rate of the Mg alloy and facilitated the new bone formation around the Mg implants. However, bioactivity, corrosion behavior, and antimicrobial performance of the Ag−Zeo−HAp coating have not been reported elsewhere. Therefore, in the present study, TiO_2 was used as an intermediate layer between the substrate and the Ag−Zeo−HAp layer to further improve the corrosion resistance of the Mg alloy when the solution passes through the overlayer. As such, the aim of the present work is to demonstrate the preparation of Ag−Zeo−HAp on the TiO_2-coated Mg alloy to improve the corrosion resistance, bioactivity, and antimicrobial performance of the substrate.

2 Experimental

The as-cast Mg−0.7Ca (mass fraction, %) alloy sample (10 mm × 10 mm × 5 mm) was prepared under protective gas atmosphere (60%Ar−40%CO_2) in an induction furnace, subsequently the ingots were ground with 320−2000 grit SiC papers until all scratches were removed according to previous study [27]. For PVD coating of the Mg alloy samples, a hybrid ion beam deposition system (HVC Penta Vacuum) which is composed of a linear ion source and magnetron sputtering source with a TiO_2 (99.99%) target was used. The parameters of PVD coating are presented in Table 1. The HAp coating was deposited on the Mg alloy by the electrodeposition method using a conventional cell including the graphite rod and the Mg alloy sample as the anode and the cathode, respectively according to the pervious study [15]. The commercial nano-ZSM-5 type Zeo ($Na_nAl_nSi_{96-n}O_{192}\cdot 16H_2O$, $0<n<27$) was exchanged through soaking 3 g of Zeo in its sodic form in 60 mL of 0.1 mol/L $AgNO_3$ aqueous solution at 70 °C for 12 h under magnetic stirring to acquire Ag−Zeo. Afterwards, the HAp-coated samples were immersed in the solution for 3 h to introduce Ag−Zeo into the HAp structure. To conduct electrochemical measurements with PARSTAT 2263 potentiostat/galvanostat (Princeton Applied Research), bare Mg alloy sample and Mg-coated samples with a surface area of 1 cm^2 were prepared and soaked in the three-electrode cell containing Kokubo SBF solution at 37 °C with a pH value of 7.44 according to Ref. [15]. Electrochemical impedance spectroscopy (EIS; Versa STAT 3) measurement was performed in the frequency range from 100 kHz to 0.01 Hz with 10 points per decade and a 10 mV. For the immersion test, the same samples were submerged into 200 mL of Kokubo SBF solution [28] (pH 7.4) according to ASTM: G1-03. The change in the pH value of the SBF was recorded all over the immersion test after every 24 h interval. The bare Mg alloy and coated alloys were immersed in Kokubo SBF solution (Table 2) for 3, 7 and 14 d and eventually cleaned with chromium trioxide (CrO_3) to eliminate the corrosion product from the specimen surface. The in-vitro corrosion rates (C_R) were subsequently measured (mm/year) using mass loss test based on the following equation: $C_R=W/(Atd)$, where W and A are mass loss and sample area exposed to solution, respectively, and t and d are exposure time and density, respectively. The release of magnesium ions from the samples was monitored by using an inductively coupled plasma spectrometry.

Table 1 Deposition parameters of PVD TiO_2 coating

Parameter	Value
Ar flow rate/(mL·min^{-1})	175
Base pressure of chamber/Pa	2.55×10^{-3}
Sputtering pressure/Pa	0.24
RF sputtering power/W	200
Deposition time/min	90
Bias voltage/V	−150

Table 2 Chemical composition of Kokubo simulated body fluid (SBF) compared to human blood plasma (mmol/L)

Na^+	K^+	Ca^{2+}	Mg^{2+}	HCO_3^-	Cl^-	HPO_4^{2-}	SO_4^{2-}
142.0	5.0	2.5	1.5	4.2	147.8	1.0	0.5

Antibacterial activity of the uncoated and coated samples against *Escherichia coli* PTCC 1330 (Gram-negative) was examined according to the disc diffusion antibiotic sensitivity and colony forming units (CFU) [29]. In the present study, gentamicin discs for bacteria (10 μg/disc) were used as reference. The bacteria were incubated at 37 °C for 24 h and the zone of inhibition (mm) around the each specimen was visually inspected. The inhibition zone (IZ) was assessed to figure out the antibacterial effect of the bare and coated samples.

An X-ray diffractometer (Siemens D5000) was used to determine the phase components using Cu K_α radiation (λ=1.5405 Å) generated at 45 kV and 40 mA. Microstructures of the bare and coated Mg alloy samples were studied by field emission scanning electron microscopy (FE−SEM, JEOL JSM−6380LA) coupled with EDX (JEOL Inc., Tokyo, Japan), and transmission electron microscopy (TEM, HT7700 Hitachi).

3 Results and discussion

3.1 Microstructure and composition

Figure 1 depicts FE-SEM images of the bare alloy and TiO_2-coated specimens. The Mg−Ca alloy microstructure contains α-Mg grains with a great amount of second phases which are distributed at the grain boundaries (Fig. 1(a)). The corresponding EDS and XRD analyses suggest that the secondary phases are Mg_2Ca (Figs. 1(a) and 2(a)). The FE-SEM images (Fig. 1(b))

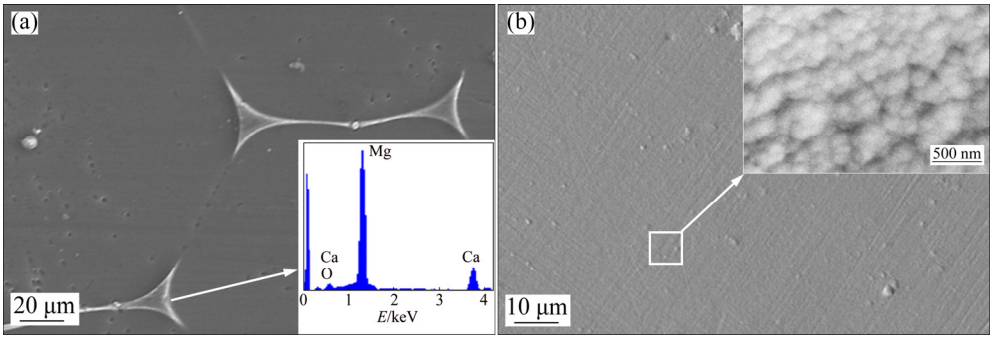

Fig. 1 FE-SEM images of surface of bare Mg alloy (a) and TiO_2-coated specimen (b)

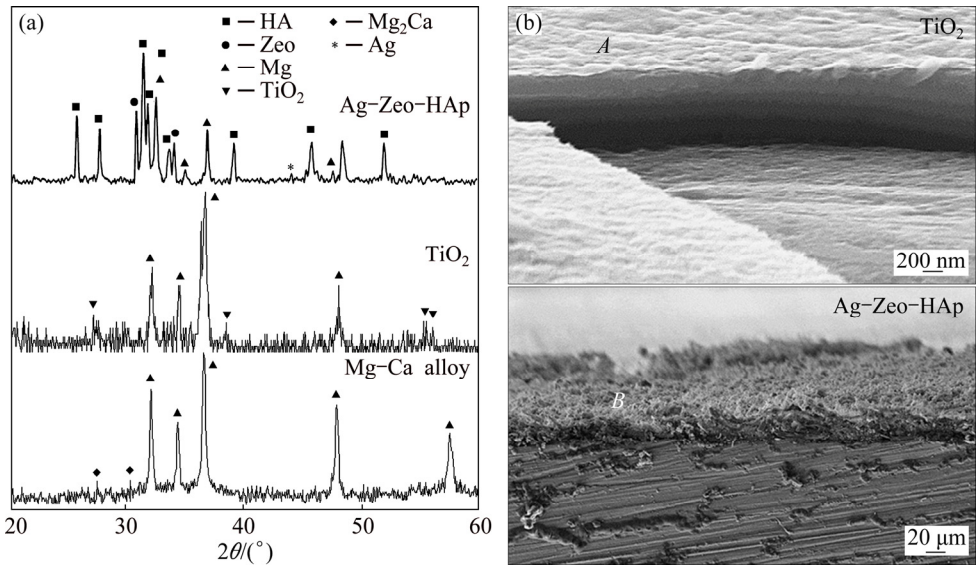

Fig. 2 XRD patterns of bare Mg−Ca alloy and TiO_2-coated specimens (a), and cross sectional FE-SEM micrographs of TiO_2-coated and Ag−Zeo−HAp-coated specimens (b)

showed that the surface of TiO_2 coating was composed of nano-scale spherical particles and their morphology was related to the coating technique and the operating conditions. The formation of TiO_2 on the surface of the alloy was proved by the EDS and XRD analyses due to the presence of the dominant peak of rutile TiO_2 (110) in addition to anatase (101) and (004), as can be seen in Figs. 2 and 3(e). However, the FE-SEM images of the Ag−Zeo−HAp coating demonstrated dense and spherical-like structures which covered the entire surface of the TiO_2-coated Mg alloy (Figs. 3(a) and (b)). The high magnification images (Figs. 3(c) and (d)) showed the formation of some spherical particles that appeared to be agglomerates accompanied by some irregular elongated agglomerates and cubic shapes. The EDS analysis obviously showed the existence of Ca, Mg, P, O, Al, and Si in the Ag−Zeo−HAp samples, as shown in Fig. 3(f), verifying that no additional elements were observed in the structure. The cross sectional FE-SEM image indicated that the TiO_2 PVD coating as the intermediate layer possesses a columnar structure with a thickness of 900 nm−1 μm (Fig. 2(b)). The TiO_2 coating presented strength bonding with the substrate owing to the formation of oxo bridges (Ti—O—Mg) which resulted in the increase of its corrosion resistance and the avoidance of the coating delamination when TiO_2-coated specimens were exposed to the corrosive solution. The Ag−Zeo−HAp coating as a top-layer is uniform without delamination at the interface with a thickness about 15 μm which can provide more effective protectiveness of the substrate (Fig. 2(b)). The TEM images (Figs. 4(a) and (b)) exhibited that the Zeo particles possess spherical-like and cubic-like shapes which are fused together, seeming as hard agglomerates with particle sizes of 340−370 nm. The round particles with a non-uniform particle size (80−90 nm) were considered to be HAp. The TEM images in the frame show that TiO_2 particles possess spherical shapes with a particle size of 30−40 nm. The XRD pattern of Ag−Zeo doped HAp exhibited the obvious peaks of HAp according to the (JCPDS No. 09-0432). The Zeo peaks appeared at 31.1° and 34.5° (JCPDS No. 38-0239), while the presence of

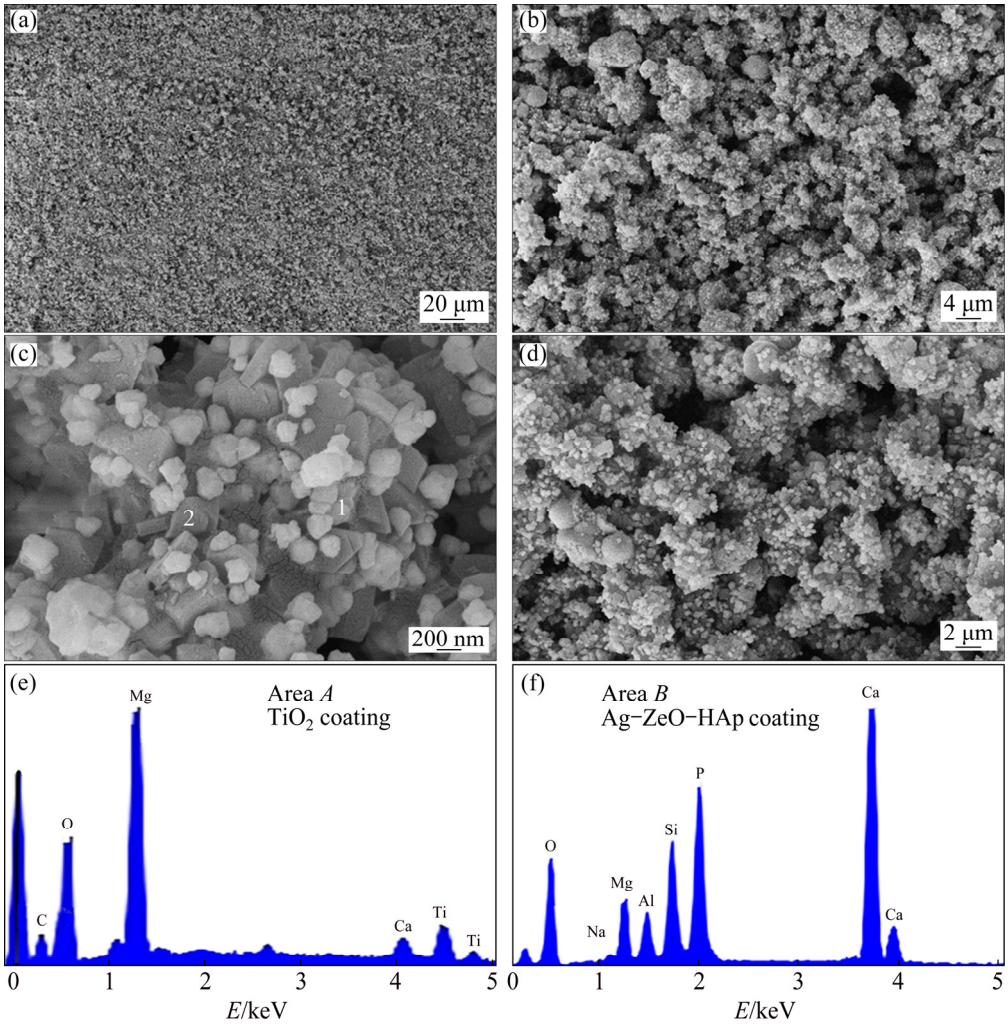

Fig. 3 FE-SEM images of surface of Ag−Zeo−HAp-coated specimens (a−d) and EDS analysis of Area *A* (e) and Area *B* (f) from Fig. 2(b)

diffraction peaks at around 44.5° was related to the (200) plane of Ag incorporation (JCPDS No. 04-0784), as shown in Fig. 2(a).

3.2 Electrochemical studies

The polarization curve of the bare and coated samples indicated that the Ag−Zeo−HAp coating presented higher corrosion potential, φ_{corr} (−1540 mV (vs SCE), the same below) compared with the TiO_2-coated (−1749 mV) and bare (−2084 mV) samples, as shown in Fig. 5(a). Additionally, from the curve it can be seen that Ag−Zeo−HAp possesses lower corrosion current density, J_{corr} (0.7 μA/cm^2) than the TiO_2-coated (52.4 μA/cm^2) and bare (193.1 μA/cm^2) samples. This illustrates that the Ag−Zeo−HAp coating decreases the cathodic process and considerably postpones the anodic process [8]. The presence of defects such as pinholes and micro-cracks in the TiO_2 PVD coating resulted in the acceleration of anodic dissolution of Mg alloy when it is exposed to the solution after a short time [2,8,30]. However, after Ag−Zeo−HAp coating, the cathodic hydrogen evolution reaction of Mg corrosion can be effectively suppressed, hence, the overall corrosion resistance will increase. One of the effective ways to investigate the kinetics of the corrosion process is the EIS test. According to the Nyquist plots (Fig. 5(b)), all samples exhibited the single

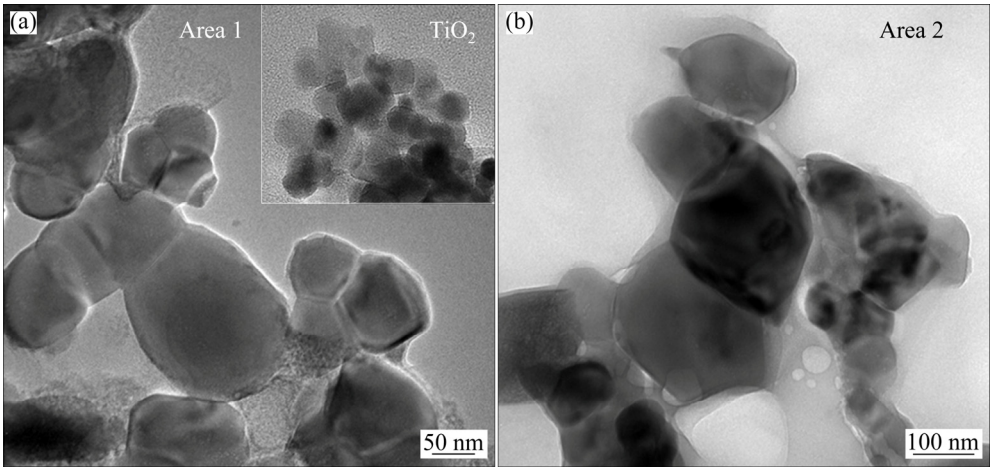

Fig. 4 TEM image of Ag−Zeo−HAp-coated specimen from Area 1 (a) and Area 2 (b) from Fig. 3(c) (Image in framed area represents TiO_2 coating)

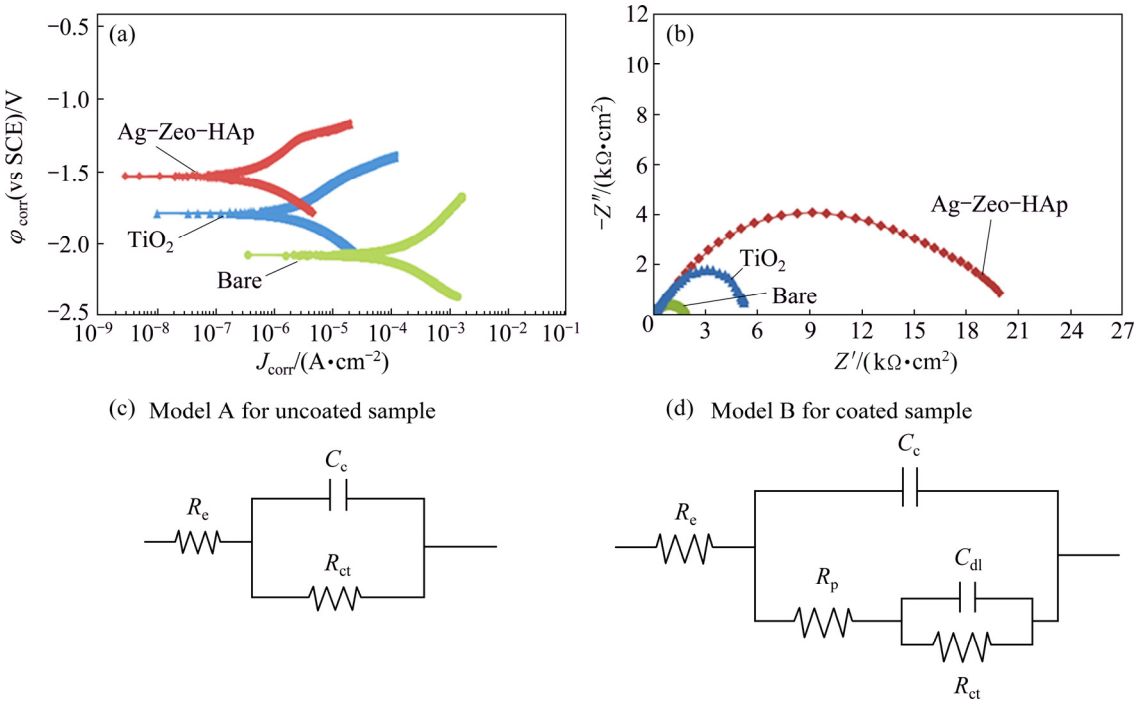

Fig. 5 Potentiodynamic polarization curves (a), electrochemical impedance spectroscopy measurements (b) and equivalent electrical circuits of bare Mg alloy (c), TiO_2-coated and Ag−Zeo−HAp-coated (d) specimens after immersion in SBF solution

capacitive loop in high frequency region with different loop sizes. It can be observed that the Ag−Zeo−HAp coating shows larger diameter than the TiO_2 coating and bare alloy, implying that the formation of a dense, compact, and thick Ag−Zeo−HAp coating layer can effectively protect the Mg alloy substrate against corrosion, particularly in the presence of the TiO_2 film as an intermediate layer.

The equivalent circuit was employed to fit the impedance spectra, where R_e, C_c, and C_{dl} are the solution resistance, coating capacitance, and double layer capacitance, respectively, and R_{ct} is the charge transfer resistance, which is related to the electrochemical corrosion rate. The equivalent circuits in Model A and Model B were used to characterize the uncoated and coated samples, respectively (Figs. 5(c) and (d)). The charge transfer resistances (R_{ct}) of the Ag−Zeo−HAp and TiO_2 coatings and bare alloy were 20.52, 5.12 and 1.32 $k\Omega \cdot cm^2$, respectively. This indicated that the corrosion resistance of Mg alloy substantially increased after deposition of Ag−Zeo−HAp over the TiO_2 film since a physical barrier is afforded through the Ag−Zeo−HAp coating by filling the porosities of the TiO_2 coating.

3.3 In-vitro bioactivity

FE-SEM images and the corresponding EDS analysis of the bare and coated Mg alloy samples after soaking in the SBF solution are shown in Fig. 6. As can be seen in Fig. 6(a), a thick corrosion product layer accompanied by cracks is formed on the surface of the bare alloy, which is attributed to the high activity of Mg bare alloy when it is directly exposed to the solution [31].

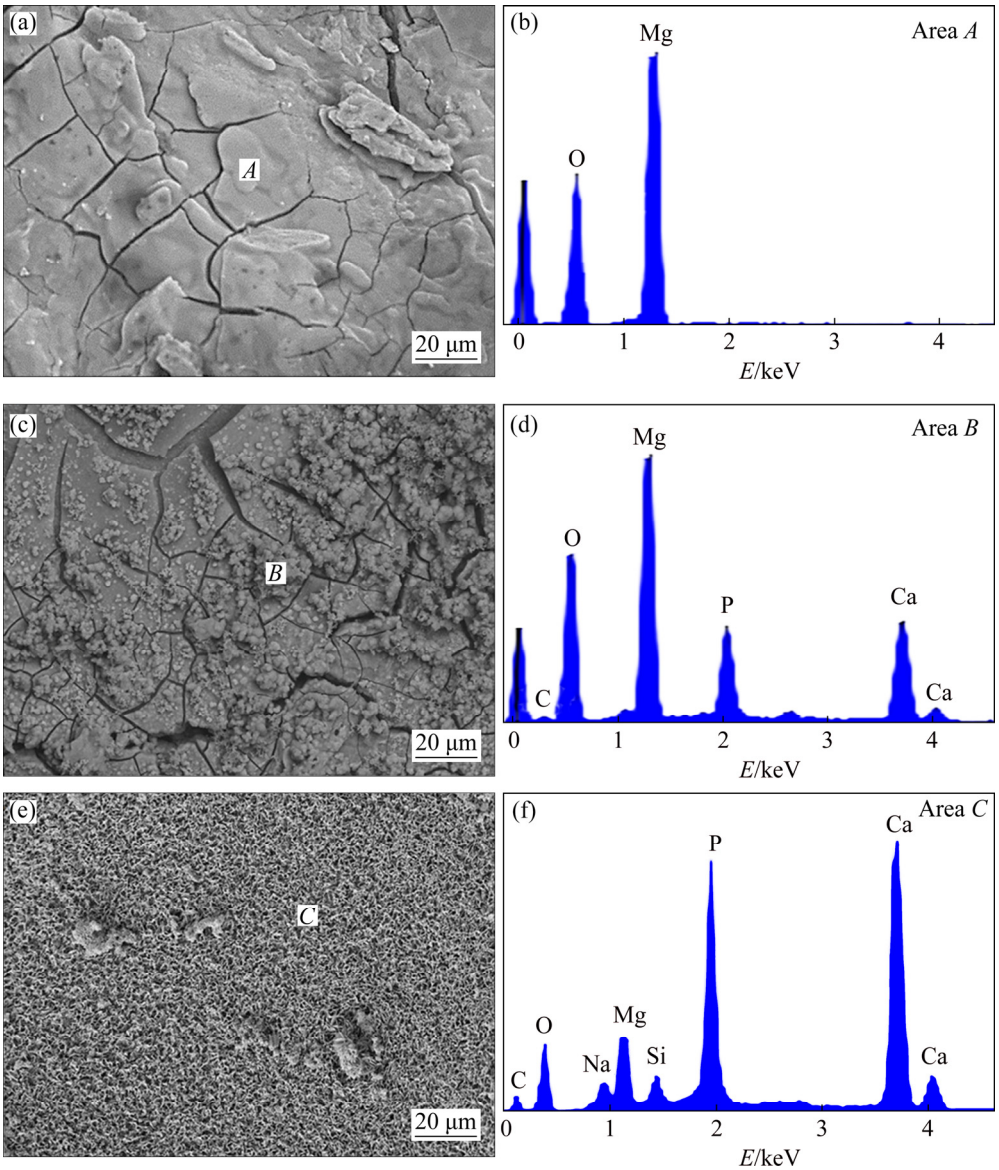

Fig. 6 FE-SEM micrographs of bare Mg alloy (a), TiO_2-coated specimen (c) and Ag−Zeo−HAp-coated (e) specimens after immersion in SBF solution, and EDS analysis of Area *A* (b), Area *B* (d) and Area *C* (f)

The EDS analysis depicted the existence of Mg and O, implying the formation of $Mg(OH)_2$. However, the surface of TiO_2 was covered with spherical-shaped particles accompanied by cracks (Fig. 6(c)). The formation of cracks on the surface is attributed to the dehydration shrinkage [31]. A homogenous plate-shaped layer with open network structure was formed on the surface of the Ag−Zeo−HAp specimen (Fig. 6(e)). The existence of Ca and P confirmed by EDS analysis exhibited the deposition of HAp on the surface of TiO_2-coated sample after immersion. However, the presence of Si besides Ca and P indicates the formation of $CaSiO_3$ and HAp on the surface of Ag−Zeo−HAp [32]. The contents of P and Ca elements will increase after Ag−Zeo−HAp coating, suggesting more deposition of HAp. SÁNCHEZ et al [32] reported that high bioactivity of zeolite functionalized by Ag or Zn is attributed to the formation of a thick HAp layer with high crystallinity after 21 d of soaking in SBF. A similar study exhibited that a considerably great amount of HAp was deposited in the Ag−nano-Zeo matrix after soaking in SBF due to the formation of a large surface area and a great amount of surface silanol groups [17]. The presence of a great amount of surface silanol groups and ion-exchange sites facilitates the attraction of Ca^{+} and PO_4^{3-} ions from the SBF solution to the surface of the Ag−Zeo−HAp coating.

The pH change in the SBF solution with uncoated and coated samples incubated for 240 h is indicated in Fig. 7(a). The graph shows that the pH values of the coated samples are lower compared with those of the uncoated one during whole immersion process. It is obvious that the presence of the Ag−Zeo−HAp as the top layer and the TiO_2 as the inner layer caused a reduction in pH during the immersion in the SBF and alleviated the local alkalisation of the Mg alloy.

A similar trend was observed for the mass loss test (Fig. 7(b)) since both coated samples presented a lower corrosion rate compared with the uncoated sample. From the graph, it can be observed that the mass loss values of the bare, TiO_2-coated, and Ag−Zeo−HAp-coated samples were 0.80, 0.62, and 0.41 mm/a (here, "a" stands for year), respectively, which indicates that the uncoated sample presented the highest degradation rate, while the TiO_2/Ag−Zeo−HAp duplex coating showed the lowest degradation rate. This phenomenon indicated that the duplex coating containing the Ag−Zeo−HAp played an essential role in providing effective protection of the Mg substrate against corrosion. Since the Ag−Zeo−HAp outer layer provides the first protection by filling the porosity of the inner layer, when the top layer becomes less effective and the solution reaches the inner layer, the TiO_2 film provides a second line of protection; thus, the corrosion resistance is significantly improved.

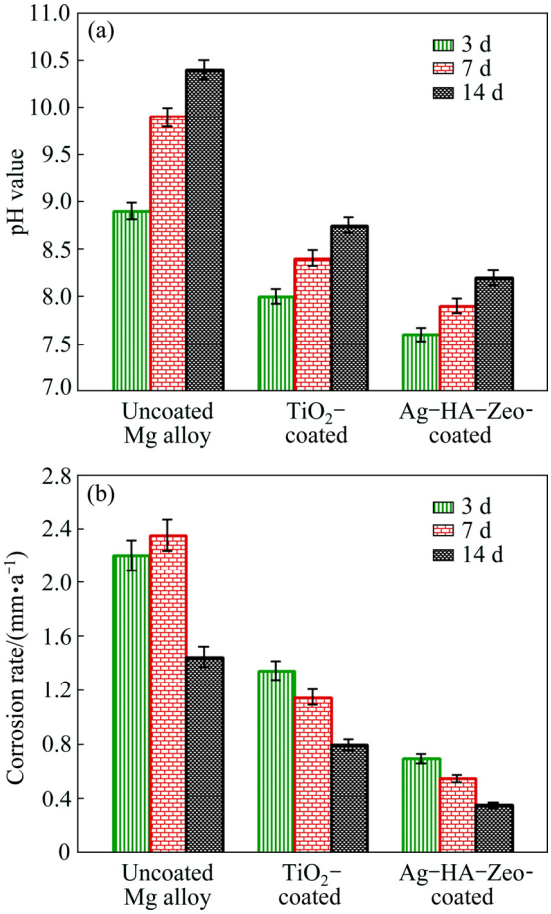

Fig. 7 pH value (a) and corrosion rate (b) for uncoated Mg alloy, TiO_2-coated and Ag−Zeo−HAp-coated Mg alloy samples in SBF solution

3.4 In vitro antibacterial activity assay

The antibacterial activity of the bare alloy and TiO_2 and Ag−Zeo−HAp coatings towards *E. coli* was evaluated. Figures 8(a−c) show the presence of the inhibition zone around the bare alloy (1.57 mm) and TiO_2 coating (2.61 mm), while a substantial inhibition halo (3.86 mm) is found for the Ag−Zeo−HAp coating. According to the SNV 1959−1992 standard, the existence of the inhibition halo more than 1 mm demonstrates the high antibacterial performance of the specimen [19]. The antibacterial property was also evaluated via CFU assay of *E. coli* as shown in Figs. 8(d−g). It can be observed that the large amount of *E. coli* colony was found in the bacterium medium agar petri dish containing the bare alloy specimen. However, the amount of *E. coli* colony after TiO_2 and Ag−Zeo−HAp deposition is reduced to about 71% and 94%, respectively, indicating their high antibacterial performance. This is due to the presence of the Zeo and Ag ions, which indicates their outstanding ability to hinder the bacterial growth. In this respect, Ag ions are considered to hinder bacterial enzymes, interfere with electron transport, and bind to DNA [16]. A different

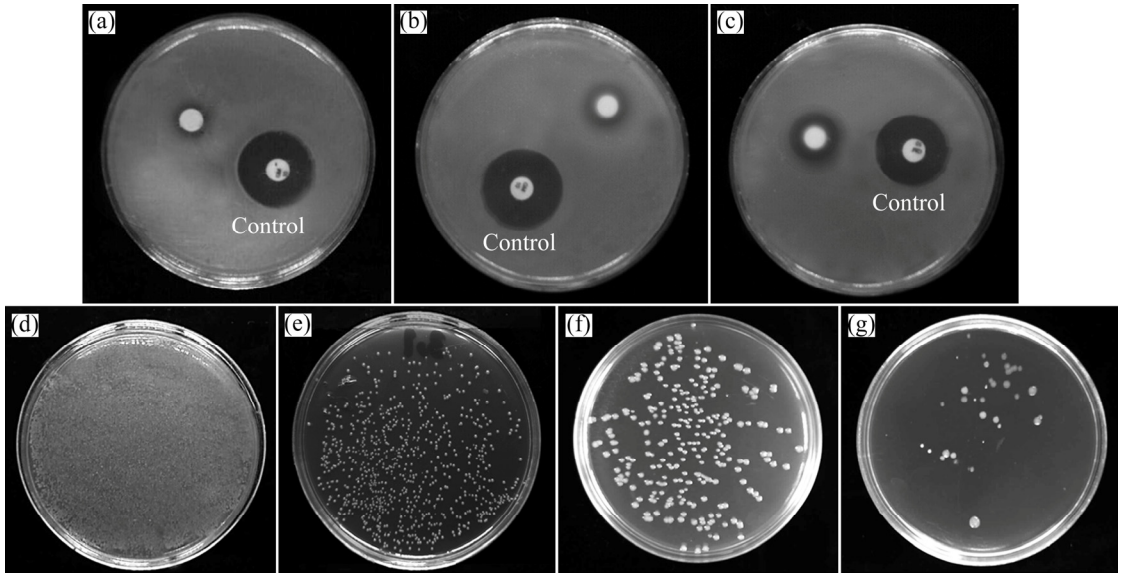

Fig. 8 Inhibition zones of bare Mg alloy (a), TiO_2-coated (b) and Ag−Zeo−HAp-coated (c) specimens, and antibacterial experiment photographs of control (d), bare Mg alloy (e), TiO_2-coated Mg alloy (f), and Ag−Zeo−HAp-coated (g) specimens against *E. coli* bacteria for 24 h

mechanism was suggested to describe the inhibitory effect of Ag−Zeo−HAp coating [19]. The antibacterial performance of Ag−Zeo−HAp is mainly dependent on the generation of silver ions which could deteriorate the cell membrane and interact with intracellular contents [33]. The Ag^+ also induces the generation of hydroxyl radicals, resulting in denature proteins, lipids, and DNA and, eventually, destroying the bacteria [33]. Another study suggested that the presence of Ag^+ ions is crucial for antimicrobial performance. The electrostatic attraction between the negatively charged cell membrane and the positively charged Ag^+ interferes with the permeability of the membrane [16,34]. Hence, the incorporation of Ag^+ leads to better interaction between Zeo and bacteria, consequently resulting in further inhibition of microorganisms.

4 Conclusions

The Ag−Zeo−HAp coating with dense spherical-like structures was formed on the TiO_2-coated Mg alloy through PVD and electrodeposition methods. The obtained results indicated that Ag−Zeo−HAp coating with antibacterial activity can provide appropriate sites for the deposition of HAp in SBF which makes strong bonds with the matrix of the natural bone and might accelerate the bone healing procedure. The electrochemical test depicted that Ag−Zeo−HAp coating increases the corrosion resistance of the TiO_2-coated Mg alloy due to the formation of a compact and uniform film with 15 μm in thickness which can block the pores and cracks of TiO_2. The antibacterial activity of the TiO_2-coated Mg alloy towards *E. coli* significantly increases after deposition of Ag−Zeo−HAp due to the existence of silver in the coating. The Ag−Zeo−HAp coating presented high corrosion resistance and good antibacterial properties, thus it can be used for other active substrates.

Acknowledgments

The authors would like to thank the Universiti Teknologi Malaysia (UTM) for providing facilities for this research.

References

[1] LIU Y C, LIU D B, ZHAO Y, CHEN M F. Corrosion degradation behavior of Mg−Ca alloy with high Ca content in SBF [J]. Transactions of Nonferrous Metals Society of China, 2015, 25: 3339−3347.

[2] CUI L Y, XU J, LU N, ZENG R C, ZHANG F. In vitro corrosion resistance and antibacterial properties of layer-by-layer assembled chitosan/poly-*L*-glutamic acid coating on AZ31 magnesium alloys [J]. Transactions of Nonferrous Metals Society of China, 2017, 27: 1081−1086.

[3] ZHENG Y F, GU X N, WITTE F. Biodegradable metals [J]. Materials Science and Engineering R, 2014, 77: 1−34.

[4] WANG X, NIE Q D, MA X L, FAN J L, YAN T L, LI X L. Microstructure and properties of co-continuous (β-TCP+MgO)/Zn−Mg composite fabricated by suction exsorption for biomedical applications [J]. Transactions of Nonferrous Metals Society of China, 2017, 27: 1996−2006.

[5] WITTE F, HORT N. Degradable biomaterials based on magnesium corrosion [J]. Current Opinion in Solid State and Materials Science, 2008, 12: 63−72.

[6] BAKHSHESHI-RAD H R, IDRIS M H, KADIR M R A, DAROONPARVAR M. Effect of fluoride treatment on corrosion

behavior of Mg−Ca binary alloy for implant application [J]. Transactions of Nonferrous Metals Society of China, 2013, 23: 699−710.

[7] ZOMORODIAN A, SANTOS C, CARMEZIM M J, SILVA T M, FERNANDES J C S, MONTEMOR M F. “In-vitro” corrosion behaviour of the magnesium alloy with Al and Zn (AZ31) protected with a biodegradable polycaprolactone coating loaded with hydroxyapatite and cephalexin [J]. Electrochimica Acta, 2015, 179: 431−440.

[8] SONG D, JING X, WANG J, WANG Y, YANG P, ZHAO M, ZHANG M. Corrosion-resistant ZSM-5 zeolite coatings formed on Mg−Li alloy by hot-pressing [J]. Corrosion Science, 2011, 53: 1732−1737.

[9] ZHAO Y B, SHI L Q, CUI L Y, ZHANG C L, LI S Q, ZENG R C, ZHANG F, WANG Z L. Corrosion resistance of silane-modified hydroxyapatite films on degradable magnesium alloys [J]. Acta Metallurgica Sinica (English Letters), 2018, 31: 180−188.

[10] ZENG R C, CUI L Y, JIANG K, LIU R, ZHAO B D, ZHENG Y F. In vitro corrosion and cytocompatibility of a microarc oxidation coating and poly(lactic acid) composite coating on Mg−1Li−1Ca alloy for orthopedic implants [J]. ACS Applied Materials & Interfaces, 2016, 8: 10014−10028.

[11] ZENG R C, LIU L J, LUO K J, SHEN L, ZHANG F, LI S Q, ZOU Y H. In vitro corrosion and antibacterial properties of layer-by-layer assembled GS/PSS coating on AZ31 magnesium alloys [J]. Transactions of Nonferrous Metals Society of China, 2015, 25: 4028−4039

[12] SUN Y H, WANG R C, PENG C Q, FENG Y, YANG M. Corrosion behavior and surface treatment of superlight Mg−Li alloys [J]. Transactions of Nonferrous Metals Society of China, 2017, 27: 1455−1475.

[13] ZENG R C, QI W C, CUI H Z, ZHANG F, LI S Q, HAN E H. In vitro corrosion of as-extruded Mg−Ca alloys—The influence of Ca concentration [J]. Corrosion Science, 2015, 96: 23−31.

[14] CUI L Y, ZENG R C, GUAN S K, QI W C, ZHANG F, LI S Q, HAN E H. Degradation mechanism of micro-arc oxidation coatings on biodegradable Mg−Ca alloys: The influence of porosity [J]. Journal of Alloys and Compounds, 2017, 695: 2464−2476.

[15] BAKHSHESHI-RAD H R, IDRIS M H, KADIR M R A. Synthesis and in vitro degradation evaluation of the nano-HA/MgF_2 and DCPD/MgF_2 composite coating on biodegradable Mg−Ca−Zn alloy [J]. Surface & Coatings Technology, 2013, 222: 79−89.

[16] SALIM M M, MALEK N A N N. Characterization and antibacterial activity of silver exchanged regenerated NaY zeolite from surfactant-modified NaY zeolite [J]. Materials Science and Engineering C, 2016, 59: 70−77.

[17] KAUR B, SRIVASTAVA R, SATPATI B, KONDEPUDI K K, BISHNOI M. Biomineralization of hydroxyapatite in silver ion-exchanged nanocrystalline ZSM-5 zeolite using simulated body fluid [J]. Colloids and Surfaces B: Biointerfaces, 2015, 135: 201−208.

[18] IQBAL N, KADIR M R A, IQBAL S, IZWAN S, RAFIQUE M S, BAKHSHESHI-RAD H R, IDRIS M H, KHATTAK M A, RAGHAVENDRAN H R B, ABBAS A A. Nano-hydroxyapatite reinforced zeolite ZSM composites: A comprehensive study on the structural and in vitro biological properties [J]. Ceramics International, 2016, 42: 7175−7182.

[19] SÁNCHEZ M J, MAURICIO J E, PAREDES A R, GAMERO P, CORTÉS D. Antimicrobial properties of ZSM-5 type zeolite functionalized with silver [J]. Materials Letters, 2017, 191: 65−68.

[20] KATARIYA M N, JANA A K, PARIKH P A. Corrosion inhibition effectiveness of zeolite ZSM-5 coating on mild steel against various organic acids and its antimicrobial activity [J]. Journal of Industrial and Engineering Chemistry, 2013, 19: 286−291.

[21] BANERJEE C P, WOO P R, GRAYSON M S, MAJUMDER A, RAMAN K R. Influence of zeolite coating on the corrosion resistance of AZ91D magnesium alloy [J]. Materials, 2014, 7: 6092−6104.

[22] CUI L Y, QIN P H, HUANG X L, YIN Z Z, ZENG R C, LI S Q, HAN E H, WANG Z L. Electrodeposition of TiO_2 layer-by-layer assembled composite coating and silane treatment on Mg alloy for corrosion resistance [J]. Surface and Coatings Technology, 2017, 324: 560−568.

[23] ZENG R C, HU Y, ZHANG F, HUANG Y D, WANG Z l, LI S Q, HAN E H. Corrosion resistance of cerium-doped zinc calcium phosphate chemical conversion coatings on AZ31 magnesium alloy [J]. Transactions of Nonferrous Metals Society of China, 2016, 26: 472−483.

[24] van PHUONG N, GUPTA M, MOON S. Enhanced corrosion performance of magnesium phosphate conversion coating on AZ31 magnesium alloy [J]. Transactions of Nonferrous Metals Society of China, 2017, 27: 1087−1095.

[25] LI X, WENG Z, YUAN W, LUO X, WONG H M, LIU X, WU S, YEUNG K W K, ZHENG Y, CHU P K. Corrosion resistance of dicalcium phosphate dihydrate/poly(lactic-co-glycolic acid) hybrid coating on AZ31 magnesium alloy [J]. Corrosion Science, 2016, 102: 209−221.

[26] WANG H, GUAN S, WANG Y, LIU H, WANG H, WANG L, REN C, ZHU S, CHEN K. In vivo degradation behavior of Ca-deficient hydroxyapatite coated Mg−Zn−Ca alloy for bone implant application [J]. Colloids and Surfaces B: Biointerfaces, 2011, 88: 254−259.

[27] BAKHSHESHI-RAD H R, HAMZAH E, DAROONPARVAR M, KAHRIZSANGI R E, MEDRAJ M. In-vitro corrosion inhibition mechanism of fluorine-doped hydroxyapatite and brushite coated Mg−Ca alloys for biomedical applications [J]. Ceramics International, 2014, 40: 7971−7982.

[28] KOKUBO T, TAKADAMA H. How useful is SBF in predicting in vivo bone bioactivity? [J]. Biomaterials, 2006, 27: 2907−2915.

[29] KOOSEHGOL S, HOSSEINABADI M E, ALIZADEH M, ZAMANIAN A. Preparation and characterization of in situ chitosan/ polyethylene glycol fumarate/thymol hydrogel as an effective wound dressing [J]. Materials Science and Engineering C, 2017, 7: 66−75.

[30] BAKHSHESHI-RAD H R, HAMZAH E, DAROONPARVAR M, YAJID M A M, ASGARANI M K, KADIR M R A, MEDRAJ M. In-vitro degradation behavior of Mg alloy coated by fluorine doped hydroxyapatite and calcium deficient hydroxyapatite [J]. Transactions of Nonferrous Metals Society of China, 2014, 24: 2516−2528.

[31] XIN Y, HUB T, CHU P K. In vitro studies of biomedical magnesium alloys in a simulated physiological environment: A review [J]. Acta Biomater, 2011, 7: 1452−1459.

[32] SÁNCHEZ M J, GAMERO P, CORTÉS D. Bioactivity assessment of ZSM-5 type zeolite functionalized with silver or zinc [J]. Materials Letters, 2012, 74: 250−253.

[33] PEREYRA A M, GONZALEZ M R, RODRIGUES T A, LUTERBACH M T S, BASALDELLA E I. Enhancement of biocorrosion resistance of epoxy coating by addition of Ag/Zn exchanged a zeolite [J]. Surface & Coatings Technology, 2015, 270: 284−289.

[34] BAKHSHESHI-RAD H R, HAMZAH E, STAIGER M P, DIAS G J, HADISI Z, SAHEBAN M, KASHEFIAN M. Drug release, cytocompatibility, bioactivity, and antibacterial activity of doxycycline loaded Mg−Ca−TiO_2 composite scaffold [J]. Materials and Design, 2018, 139: 212−221.

银–沸石掺杂羟基磷灰石镁合金涂层的生物活性、体外腐蚀行为和抗菌活性

H. R. BAKHSHESHI-RAD[1,2], E. HAMZAH[2], A. F. ISMAIL[3], M. AZIZ[3], E. KARAMIAN[1], N. IQBAL[4]

1. Advanced Materials Research Center, Department of Materials Engineering,
Najafabad Branch, Islamic Azad University, Najafabad, Iran;
2. Department of Materials, Manufacturing and Industrial Engineering,
Faculty of Mechanical Engineering, Universiti Teknologi Malaysia, 81310 Johor Bahru, Johor, Malaysia;
3. Advanced Membrane Technology Research Center (AMTEC),
Universiti Teknologi Malaysia, 81310 Skudai, Johor Bahru, Johor, Malaysia;
4. Department of Biomedical Engineering, University of Engineering and Technology, Lahore, Pakistan

摘　要：镁基合金作为临时植入材料的应用受到了越来越多的关注，然而，由于其降解速率高，因此应用受到了限制。为了降低镁合金的降解速率，本文作者采用物理气相沉积(PVD)辅助电沉积技术在镀氧化钛(TiO_2)的镁合金上涂覆掺银–沸石羟基磷灰石(Ag−Zeo−HAp)涂层。X 射线衍射(XRD)分析和场发射扫描电镜(FESEM)图片显示，在厚度约为 1 μm 的二氧化钛薄膜上形成了均匀且致密的 Ag−Zeo−HAp 涂层，厚度约为 15 μm。动电位极化(PDP)和电化学阻抗谱(EIS)测试表明，通过 Ag−Zeo−HAp 涂层，Mg−Ca 合金的耐腐蚀性大大提高。模拟体液(SBF)浸泡测试生物活性试验结果表明，在 14 d 后的 Ag−Zeo−HAp 表面上形成了一层致密且均匀的类骨磷灰石层。采用琼脂扩散法和平板涂布法对抗菌活性进行研究。结果表明，与 TiO_2 涂层的镁合金(2.61 mm)相比，Ag−Zeo−HAp 涂层对大肠杆菌(*E. coli*)的抑制区(3.86 mm)明显增大。Ag−Zeo−HAp 涂层具有良好的抗菌性能、良好的生物活性和耐腐蚀性，是生物医学应用的理想涂层材料。

关键词：镁合金；沸石；涂层；生物活性；腐蚀行为；抗菌活性

(Edited by Wei-ping CHEN)